

## Micro Cutting of Tungsten Carbides with SEM Direct Observation Method

Heo Sung-jung\*

*Department of Mechanical Engineering, Doowon Technical College  
678 Changwon-ri, Chuksan-myon, Ansong-si, Gyonggi-do 456-890, Korea*

This paper describes the micro cutting of wear resistant tungsten carbides using PCD (Poly-Crystalline Diamond) cutting tools in performance with SEM (Scanning Electron Microscope) direct observation method. Turning experiments were also carried out on this alloy (V50) using a PCD cutting tool. One of the purposes of this study is to describe clearly the cutting mechanism of tungsten carbides and the behavior of WC particles in the deformation zone in orthogonal micro cutting. Other purposes are to achieve a systematic understanding of machining characteristics and the effects of machining parameters on cutting force, machined surface and tool wear rates by the outer turning of this alloy carried out using the PCD cutting tool during these various cutting conditions. A summary of the results are as follows : (1) From the SEM direct observation in cutting the tungsten carbide, WC particles are broken and come into contact with the tool edge directly. This causes tool wear in which portions scrape the tool in a strong manner. (2) There are two chip formation types. One is where the shear angle is comparatively small and the crack of the shear plane becomes wide. The other is a type where the shear angle is above 45 degrees and the crack of the shear plane does not widen. These differences are caused by the stress condition which gives rise to the friction at the shear plane. (3) The thrust cutting forces tend to increase more rapidly than the principal forces, as the depth of cut and the cutting speed are increased preferably in the orthogonal micro cutting. (4) The tool wear on the flank face was larger than that on the rake face in the orthogonal micro cutting. (5) Three components of cutting force in the conventional turning experiments were different in balance from ordinary cutting such as the cutting of steel or cast iron. Those expressed a large value of thrust force, principal force, and feed force. (6) From the viewpoint of high efficient cutting found within this research, a proper cutting speed was 15 m/min and a proper feed rate was 0.1 mm/rev. In this case, it was found that the tool life of a PCD tool was limited to a distance of approximately 230 m. (7) When the depth of cut was 0.1 mm, there was no influence of the feed rate on the feed force. The feed force tended to decrease, as the cutting distance was long, because the tool was worn and the tool edge retreated. (8) The main tool wear of a PCD tool in this research was due to the flank wear within the maximum value of  $V_{max}$  being about 260  $\mu\text{m}$ .

**Key Words :** PCD Cutting Tools, WC-Co, SEM (Scanning Electron Microscope), Micro Cutting, Direct Observation Method, Tool Wear, Cutting Force, Machined Surface

---

\* E-mail : sjheo@doowon.ac.kr

TEL : +82-31-670-7135; FAX : +82-31-670-7035

Department of Mechanical Engineering, Doowon Technical College 678 Changwon-ri, Chuksan-myon, Ansong-si, Gyonggi-do, 456-890 Republic of Korea. (Manuscript Received June 21, 2003; Revised February 4, 2004)

### 1. Introduction

Tungsten carbides possess superior hardness and strength both at low and high temperatures due to stable physical properties. Therefore, this

alloy is one of the most difficult-to-cut materials at present, but its usage has been already broadened to every commercial application such as mining tools, wear-resistant tools and cutting tools, among others.

They are also used in cutting tools. Wear resistant tungsten carbides contain more cobalt compared to normal tungsten carbides used for cutting tools, and the grain size of the tungsten carbide is larger.

Various grinding experiments on wear resistant tungsten carbides have been previously carried out in the author's previous work. (Heo et al., 1993) The machining of tungsten carbide is mainly dependent on the grinding process because milling, turning and drilling have many difficulties. Generally, the tool materials must be over 4 times harder than the work materials so that the cutting process becomes economical. (Technical Research Institute, 1997) Recently, PCD (Poly-Crystalline Diamond) tools have been put into practical use, and the machining of the tungsten carbides is becoming gradually easier. Although there are several available technical reports regarding tool life, surface roughness and cutting force in longitudinal turning with wear resistant tungsten carbides (Technical Research Institute, 1997; 1995), knowledge and technical data are limited and do not offer enough information to understand completely the mechanics of cutting yet.

To study the possibility of the precision machining of the tungsten carbides, the relation between the cutting conditions and the finished surface was investigated by the aid of SEM observations of the micro cutting process using several kinds of tungsten carbides. In cutting the tungsten carbide with the PCD tool, the breakage behavior of tungsten carbide (WC) particles and cobalt (Co) was observed, and the tool wear was investigated in detail. Moreover the chip formation was also investigated.

These findings will focus on present cutting conditions that can obtain precise finished surfaces and reasonable machining efficiency, while at the same time minimizing tool wear.

## 2. Experimental Work

### 2.1 Orthogonal micro cutting experiment in SEM

#### 2.1.1 Experimental device

Studies have already reported on the micro cutting of several kinds of alloys with SEM device (HANASAKI et al., 1989; 1989; 1990; 1996). The micro cutting device used for this research was slightly different from previous devices, and was improved for a newly corrected establishment of depth of cut and tool holder's stiffness.

A orthogonal micro cutting device for difficult-to-cut materials such as the tungsten carbides in SEM was developed for investigating the proposed method. This apparatus is composed mainly of the work material holder, the tool holder, and a specially designed tool. Since the previously established depth of cut transferred to the wedge, repetitive errors were often made.

As new and improved devices could move the work material holder directly using a motor, the correct depth of cut within  $1\ \mu\text{m}$  could be obtained. By specifically improving the tension spring of the work material holder, the tensile load in the opposite direction of the cutting was restricted and the work material's transfer by cutting force could be stopped.

The tool holder was manufactured to change the height of the tool depending on the thickness of work material, as was the previous apparatus for fixed load. As new tool holders have the highest stiffness, the flexure deformation could be repressed in the cutting of the tungsten carbide.

#### 2.1.2 Work material/tool material and experimental conditions

The work material is V60 grade tungsten carbide that is used mainly for wear and impact resistant tools in metal mould factories. The chemical compositions are shown in Table 1. The mechanical and the thermal properties of this work material are shown in Table 2. In Table 2, as it has been established, the value of hardness and Young's modulus becomes lower as

**Table 1** Chemical composition of work material (wt%)

Composition	W	Co	C
Volume Fraction	65.3~73.7	22~30	4.3~4.7

**Table 2** Mechanical properties of tungsten carbide V60

Specific gravity (Mg/cm <sup>3</sup> )	Hardness (HRA)	Compressive Strength (Gpa)	Young's modulus ( $\times 10^4$ kg/mm <sup>2</sup> )
13.1	82.0	3.14	470

the quantity of cobalt increases. This work material was sintered and formed to the designated size (15×15×0.7 mm), and lapped after being ground on a precision grinding machining. The work material fixed on micro cutting device was cut after confirming that the degree of the vacuum reached  $2.0 \times 10^{-2}$  Pa in SEM.

During the micro cutting, the cutting was stopped at free-step and a photo was taken. One part of the cutting process was recorded with a VCR, and this was used to analyze the data.

The micro cutting tool material used for this experiment was a single polycrystalline diamond tool (PCD). The tool has the front rake angle  $\alpha$  of 0° and the relief angle  $\beta$  is 3°. In these cutting conditions, the cutting speed was 10  $\mu$ m/s, and the depth of cut was approximately 10 to 15  $\mu$ m.

The first observation of the work material focused on experimental cutting and was carried out with SEM direct observation after micro cutting at the depth of cut 10  $\mu$ m.

## 2.2 Turning experiment with CNC lathe

A 60 mm diameter  $\times$  100 mm long bar of tungsten carbide (V60), manufactured by the S Corporation of Korea was used for the turning experiments. The mechanical and chemical compositions for the work material used in this experiment are the same as those shown in Table 1 and 2.

The tool inserts are commercially available PCD and are used as a reference point. The geometric configuration of the tool insert is

**Table 3** Cylindrical Turning conditions

Cutting speed (m/min)	10, 15, 20, 30
Depth of cut (mm)	0.05, 0.1, 0.2, 0.3
Feed rate (mm/rev)	0.05, 0.1, 0.2, 0.3
Cutting method	Dry, Wet
Tool material	PCD
Tool insert	TNGA160408
Tool holder	PTGNR2525-M16

TNGA160408. The insert was attached on the tool holder, which has the cutting edge angle of 90°. The machine tool used in this experiment for continuous, dry and wet turning tests is a CNC lathe TNL-35S (SAEIL Heavy Industry, Korea) with a Sentrol-L system. The cutting fluid used was an emulsion type applied at a flow rate 10 l/min. More detailed tool geometry and cutting conditions are shown in Table 3.

The effects of the three machining parameters (cutting speed, feed rate and the depth of cut) were investigated. In order to understand the influence of individual machining parameters on the cutting force, one parameter was varied in each set of the study while all other parameters were kept constant.

The cutting forces were measured by means of a quartz piezoelectric type tool dynamometer (KISTLER, 3-Component dynamometer Type 9257B) connected to a multi-channel charge amplifier (KISTLER, Type 5019 A), a 500 MHz oscilloscope (Leroy, Type 5019 A) and a data recorder (TEAC, Type XR-310).

Surface roughness parameters were measured on a Rank Taylor Hobson (RTH) Form Talysurf Plus, both having a cut-off 0.8 mm and a sample length of 4 mm. The cutting tool wear was measured with a toolmaker's microscope.

## 3. Result and Discussion

### 3.1 Orthogonal micro cutting experiment in SEM

#### 3.1.1 SEM direct observation of micro cutting of tungsten carbide

With the use of a micro cutting apparatus, SEM

direct observation could be carried out to clarify microscopically the behavior of the work material near the cutting edge. In order to see the microstructure of WC particles before cutting, and to investigate how these particles change after cutting, Fig. 1 shows a SEM micrograph of the non-machined region which is where cutting began, about 100  $\mu\text{m}$  distance from the left end of the work material.

Figure 2 shows a SEM micrograph of the machined region at 60  $\mu\text{m}$  point after cutting. This is formed by cutting at a depth of 10  $\mu\text{m}$  and a cutting speed of 10  $\mu\text{m/s}$ . The arrow shown in Fig. 2 is the cutting direction in SEM micro cutting.

It can be seen that a WC particle of about size 5  $\mu\text{m}$  in the front part of the tool rake surface is beginning to crack. This particle exists on the right side of Fig. 1 (symbol A), but the crack had not formed before cutting.

Also, it was confirmed that this WC particle's crack had already begun in a frontward 10  $\mu\text{m}$  area of the tool cutting edge. Fig. 3 shows the growth state of the crack that has occurred to the particle after the tool displacement at about

5  $\mu\text{m}$  from Fig. 2. In Fig. 3, the crack of the WC particle grew more drastically, and the particles were mixed into a state that is difficult to see in proximity to the tool neighborhood.

What was observed next was the cutting mechanism in the orthogonal micro cutting. This observation deals with the process where primary WC particles become fine grains crushed on the shearing deformation zone.

As shown in Fig. 4(a), a particle with the size of about 10  $\mu\text{m}$  was moved to the left from Fig. 3. The WC particle shows the beginning of a crack at the point of about 3  $\mu\text{m}$  at the front of the tool, and this crack grows from the tool edge frontward. At this time, a WC particle could be observed as in Fig. 1 at the right (symbol B), but a crack has not appeared as before cutting. A crack from a small WC particle can also be seen on the right of the larger crack. As shown in Fig. 1, the crack did not happen before cutting, but progresses by the action of the tool.

The small particle did crack in the 10  $\mu\text{m}$  area from the cutting edge frontward and grows to the large particle by the cutting force. The crack grows by the progress of the cutting as shown in

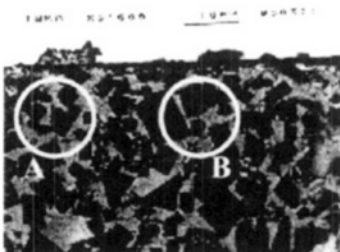


Fig. 1 SEM micrograph of non-machined region



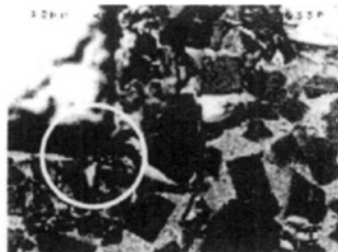
Fig. 2 SEM micrograph of the machined region



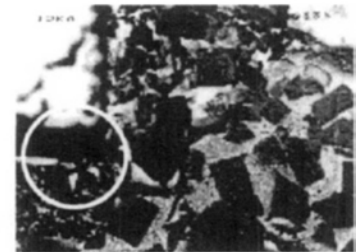
Fig. 3 SEM micrograph of typical crack formation



(a) Primary crack



(b) Growth of crack



(c) Displacement of the particle

Fig. 4 Successive SEM micrograph of tungsten carbide in orthogonal micro-cutting

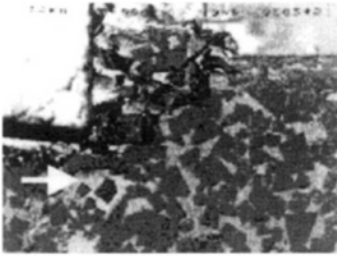


**Fig. 5** The shearing deformation zone

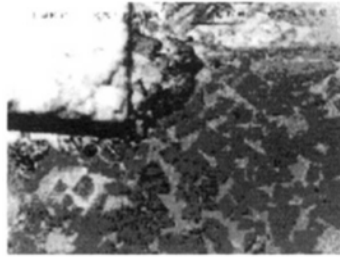


**Fig. 6** SEM micrograph of chip formation

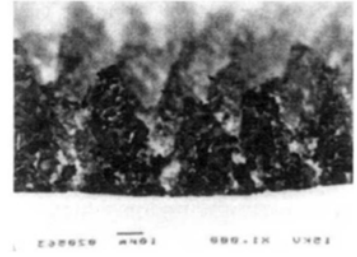


**Fig. 7** Cross section of chips formed

Fig. 4(b). The part under the particle hardly moved, and was pushed compulsorily by the cutting force. Fig. 4(c) shows that the part under the particle rotates clockwise, and collided with the cutting tool edge.

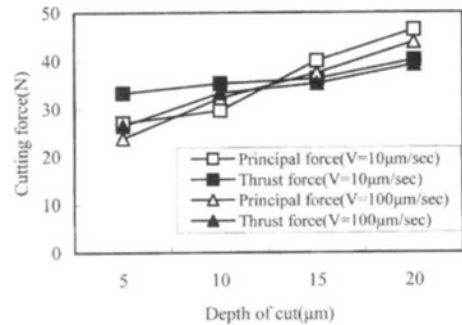
From Fig. 3 and 4, the SEM direct observation in cutting the tungsten carbide, WC particles are broken and come into contact with the tool edge directly. This causes the tool wear where a part of the tool is strongly scraped.

Figure 5 shows a SEM micrograph of the machined region at a point 200  $\mu\text{m}$  after cutting. This is formed cutting with a depth of 15  $\mu\text{m}$  and a cutting speed of 10  $\mu\text{m}/\text{s}$ . From this micrograph, a shearing deformation zone appearing upward at a slant could be seen. The WC particles on the shearing deformation zone are broken greatly. The micro cutting is gone from the zone; a chip is formed as shown in Fig. 6.

Also, Fig. 5 and 6 show that there are two chip formation types. One type of shear angle is comparatively small and the crack of the shear plane becomes wide; the other is a type of shear angle above 45 degrees and the crack of the shear plane does not widen. These differences are caused by the stress condition which gives rise to the friction at the shear plane.

Figure 7 shows a SEM micrograph of the chip formation in this time as reference.

From this SEM direct observation of micro-cutting, primary WC particles were crushed and/or fine grained in the shearing deformation zone. A part of the particles were observed to collide directly with the cutting edge of the tool following the micro cutting. This appears to be caused by severe tool wear in the turning of



**Fig. 8** Relation between cutting force and depth of cut

tungsten carbides.

### 3.1.2 Cutting forces on micro cutting of tungsten carbide

Figure 8 shows the relation between cutting force and depth of cut on micro cutting in SEM at the cutting speed rate of 10  $\mu\text{m}/\text{sec}$  and 10  $\mu\text{m}/\text{sec}$ . As can be seen in this figure, the cutting forces did not change so much within this experimental range. However the change of the thrust cutting force was shown to be different from the principal cutting force regarding depth of cut.

It seemed that the cutting speed hardly influenced the thrust force, because of the frictional force between the cutting tool edge and small WC particles at the low cutting speed on micro cutting in SEM.

As we know, the thrust cutting force occurred by the contact between the flank face and work material near the cutting edge. The flank wear did not increase so much at the primary cutting region when using a PCD cutting tool with the specific rake angle of 0 degrees.

Therefore, it may be attributed to the fact that the depth of cut is not a serious concern to the thrust cutting force in the primary cutting process. This increasing tendency of cutting forces at the primary cutting region is the same as the experimental result that was obtained for the cylindrical turning in the Fig. 14 and 15 of section 3.2.2 below.

On the other hand, the principal force was increased proportional to the depth of cut. This may indicate that the WC particles that are broken come into contact with the influence of the tool edge directly.

In the meantime, the value of surface roughness for a given cutting speed  $V=10 \mu\text{m}/\text{sec}$  and depth of cut  $t=10 \mu\text{m}$  on this work material can be obtained as follows:  $R_a=0.09 \mu\text{m}$ ,  $R_{\text{max}}=1.19 \mu\text{m}$ ,  $R_z=0.50 \mu\text{m}$ .

**3.1.3 Tool wear on micro cutting of tungsten carbide**

Fig. 9 shows a microphotograph of the tool unworn and the tool worn away on micro cutting in SEM. From this comparison, Fig. 9 shows

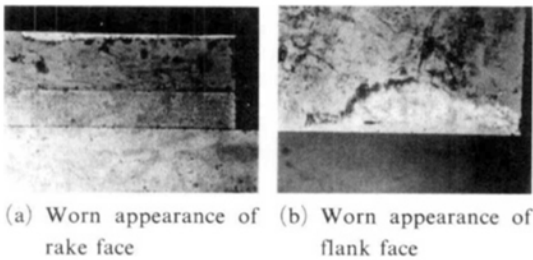


**Fig. 9** Optical microphotographs of unworn and worn appearance of PCD tool for micro-cutting

that there is tool wear due to the cutting force on the rake face and flank face. According to this observation, it can be seen that the tool wear on the flank face was larger than that on the rake face. This may be attributed to the fact that the principal cutting force was more than the thrust cutting force in the cutting of difficult-to-cut materials.

**3.2 Turning experiment in lathe**

**3.2.1 Tool wear on cylindrical turning experiment**

In order to determine the effects of cutting distance on tool wear during severe cutting conditions, the tungsten carbide was cylindrical and turned on a PCD cutting tool. Fig. 10 shows the relation between the cutting distance  $L$  and the maximum value of the flank tool wear width ( $V_{\text{max}}$ ) in the turning of tungsten carbides with the PCD tools after outer cutting at the depth of cut of 0.2 mm, cutting speed of 30 m/min and feed rate of 0.2 mm/rev. In all tool inserts shown in Fig. 10, the flank wear was roughly parallel to the cutting edge. The characteristic wear, such as the chipping and the boundary wear, were not observed.

From the above mentioned, the main tool wear of PCD tool inserts in this research was the flank tool wear within a maximum value of flank wear width  $V_{\text{max}}$  about 260  $\mu\text{m}$ . As a result of these observations, it was clear that the abrasive wear part was found on both the flank and the rake face, and adhesion was not remarkably noted.

In order to determine the wear mechanism of

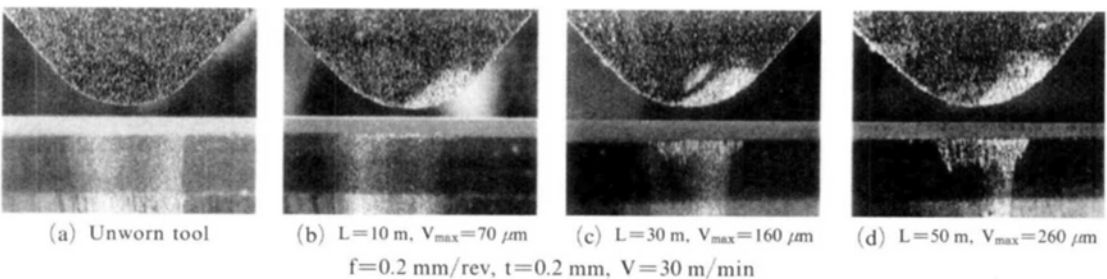


**Fig. 10** Relation between the cutting distance  $L$  and the maximum value of the flank width  $V_{\text{max}}$

PCD tools in detail, the SEM observation was carried out on the tool worn surface. Fig. 11 shows a SEM micrograph of the unworn and worn PCD tool at the depth of cut of 0.2 mm, cutting speed of 30 m/min and feed rate of 0.2 mm/rev after 6.8 m cutting. In these Figures, Fig. 11(b) and (c) show severed grooves and abrasive traces. This wear behavior is a typical abrasion, and the cause of this appearance may be that the binder of the tool is abraded by hard WC particles from the work materials, which causes diamond grains to be detached from the bond.

From these measurements, the main tool wear of PCD tool inserts in this research was the flank wear within the maximum value of the flank tool wear width  $V_{max}$  about  $260 \mu\text{m}$ . As a result of these observations, it was clear that the abrasive wear part was found on both the flank and the rake face, and adhesion is not remarkably noted.

In order to clarify the effect of cutting conditions on the tool wear in detail, the relation

between the tool wear width and the cutting distance was carried out at the cutting speed of 10 m/min and 15 m/min. The results of the experiment are shown in Fig. 12.

In this figure, the flank tool wear width parallel to the cutting distance was increased at both cutting speed ranges, and the change of cutting speed seems not to influence tool life drastically. Also, the tool life criterion was that the maximum value of the flank tool wear width was 0.3 mm. In this test, cutting was stopped at every 10 m and tool wear was measured with a micrometer-equipped microscope.

Figure 13 shows the relation between the flank tool wear width and the cutting distance at the feed rate of 0.1 mm/rev and 0.2 mm/rev and cutting speed of 10 m/min respectively.

At both a feed rate of 0.1 mm/rev and 0.2 mm/rev, the changes increase almost in proportion to the cutting distance, excluding the tool wear width as it increased rapidly in the primary cut-



(a) Unworn appearance (b) Worn appearance of rake face (c) Worn appearance of flank face

**Fig. 11** SEM micrograph of the worn appearance of PCD tool

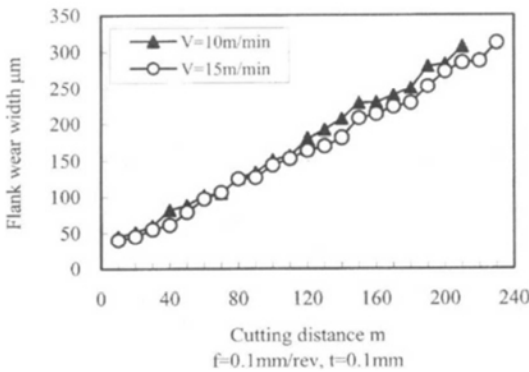


**Fig. 12** Relation between flank wear width and cutting distance

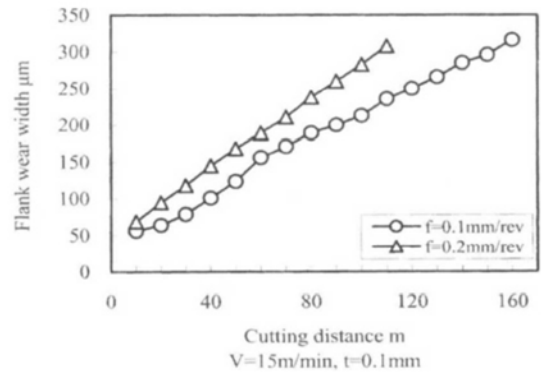


**Fig. 13** Relation between flank wear width and cutting distance

ting process. From these findings, an increasing rate at the feed rate of 0.2mm/rev was more rapidly reached than at the feed rate of 0.1 mm/rev.

If we presume from a viewpoint of high efficiency cutting and tool life within this research, a proper cutting speed was 15 m/min and a proper feed rate was 0.1 mm/rev. In this case, it was found that the tool life of PCD tool was a cutting distance up to a point of 230 m approximately.

**3.2.2 Cutting forces on turning experiment**

It is commonly expected that cutting speed is an important parameter that has a strong effect on the quality of the machined surface. The relation between the cutting force and the cutting distance at the cutting speed of 10 m/min and 15 m/min is shown in Fig. 14.

At a cutting speed of both 10 m/min and 15 m/min, the changes increased nearly in proportion to the cutting distance, but a dispersion of some amount was seen in the thrust cutting force.

In Fig. 14, the tendency was to increase the thrust cutting force at the cutting distance over 180 m and a cutting speed of 10 m/min. However the increasing tendency of the three components of cutting force did not seem so different at the range of cutting speed within this research as a whole.

At the cutting speed of 10 m/min, the thrust cutting force was approximately 20 N~300 N rather higher than the principal cutting force at the cutting distance of 70 m and 200 m. The lower

differences at a cutting speed of 20 m/min can be found.

This increasing tendency of the thrust cutting force being more evident than with the other cutting forces should be noticed. This may indicate the relation with the flank tool wear width closely as the above mentioned shown in Fig. 12.

Considering the cutting of tungsten carbide, there may be much unknown yet, but in this experiment, three components of cutting force were different in balance from ordinary cutting such as the cutting of steel or cast iron. In the cutting of tungsten carbide, namely, the feed cutting force decreases with decreasing cutting distance. Those large values were obtained by order of thrust force, principal force, feed force, and a peculiar phenomenon said to be one feature of cutting high strength materials such as tungsten carbide.

Figure 15 shows the relation between the cutting forces and the cutting distance at the feed rate of 0.1 and 0.2 mm/rev. At both feed rates, the increasing tendency of three components of cutting force was parallel in their increase of cutting distance, but the principal force and the thrust force increased rapidly at the feed rate of 0.2 mm/rev. It can be determined once again that the feed rate of 0.1 mm/rev was a more suitable condition than the feed rate of 0.2 mm/rev in the cutting of tungsten carbide for the conditions under Fig. 13.

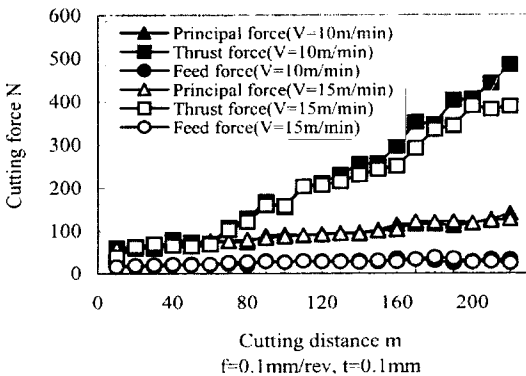


**Fig. 14** Relation between cutting force and cutting distance

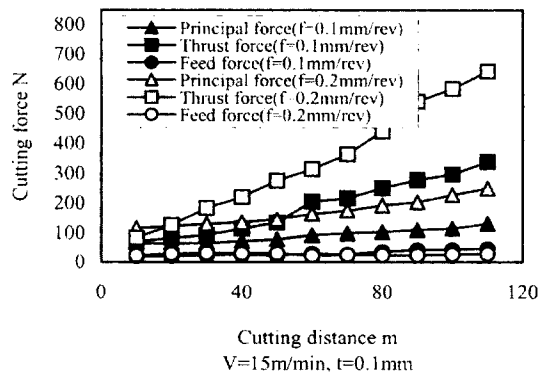


**Fig. 15** Relation between cutting force and cutting distance



The thrust force was observed as being especially fast in primary cutting distance within 10 m. This shows that the feed rate is one of most important factors among the cutting parameters in the cutting of tungsten carbide. This machining characteristic may indicate one reason which promotes the progress of the tool wear.

On the other side, the feed force was measured to be smaller rather at the cutting distance over the 80 m and the feed rate of 0.2 mm/rev. This suggests that the depth of cut appeared to affect the feed force significantly.

What was not expected was the lack of influence of the feed rate on the feed force when the depth of cut was 0.1 mm. The feed force tended to decrease as the cutting distance was lengthened because the tool was worn and the tool edge retreated.

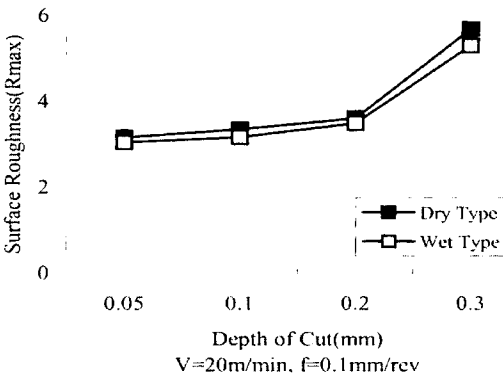


Fig. 16 Relation between cutting force and depth of cut

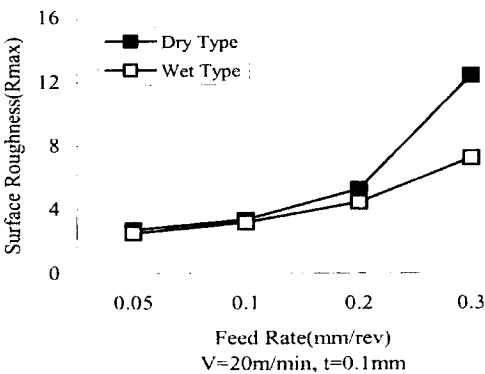


Fig. 17 Relation between cutting force and feed rate

### 3.2.3 Surface roughness on turning experiment

Figures 16 and 17 show the relationship between the surface roughness and cutting parameter. It is commonly expected that the smaller the feed rate and the depth of cut, the smoother the machining surface. However as shown in these figures, the surface roughness has a weak relationship with the depth of cut. Although the increment of the depth of cut causes an increase of cutting force, traverse feed does not change. Once again the feed rate is a more important factor than cutting speed or the depth of cut in the cutting of tungsten carbide.

In these cases, as explained, it can be seen that the cutting fluid used in this experiment had less influence on the cutting of tungsten carbide.

## 4. Conclusion

Based on these experimental results, the following conclusions can be drawn :

(1) From the SEM direct observation in cutting the tungsten carbide, WC particles are broken and come into contact with the tool edge directly. This causes tool wear and a strong scraping against the tool.

(2) There are two chip formation types. One is the type where the shear angle is comparatively small and the crack of the shear plane widens ; the other is the type where the shear angle is above 45 degrees and the crack of the shear plane does not become wide. These differences are caused by the stress condition which gives rise to the friction at the shear plane.

(3) The thrust cutting forces tend to increase more rapidly than the principal forces, as the depth of cut and the cutting speed are increased preferably in the orthogonal micro cutting.

(4) The tool wear on the flank face was larger than that on the rake face in the orthogonal micro cutting.

(5) Three components of cutting force in the conventional turning experiments were different in balance from the ordinary cutting such as that cutting of steel or cast iron. Those expressed a larger value by order of thrust force, principal

force, feed force.

(6) If we presume from a viewpoint of high efficiency cutting within this research, a proper cutting speed was 15 m/min and a proper feed rate was 0.1 mm/rev. In this case, it was found that the tool life of PCD tool was a cutting distance of approximately 230 m.

(7) When the depth of cut was 0.1 mm, there was no influence of the feed rate on the feed force. The feed force tended to decrease as the cutting distance became longer because the tool was worn and the tool edge retreated.

(8) The main tool wear of PCD tool inserts in this research was the flank wear within the maximum value of the flank wear width  $V_{\max}$  of approximately 260  $\mu\text{m}$ .

## References

- Hanasaki, S., Touge, M., Tanokubo, E. and Hasegawa, Y., 1989, "In situ observation of micro cutting of Al-Si alloy by using scanning electron microscope," *Journal of Japan Institute of Light Metals*, Vol. 39, No. 10, pp. 705~709.
- Hanasaki, S., Touge, M. and Tsukuda, I., 1989, "Study on cutting of Al-Si alloys," *Japan Society of Precision Engineering*, Vol. 55, No. 06, pp. 1091~1096.
- Hanasaki, S., Touge, M., Miyamoto, T. and Fujiwara, J., 1990, "Study on cutting mechanism of fiber reinforced metals (1st Report)", *Japan Society of Precision Engineering*, Vol. 56, No. 12, pp. 2225~2230.
- Hanasaki, S., Fujiwara, J. and Miyamoto, T., 1996, "Measurement of strain rate near cutting edge by image processing on micro cutting commercially pure aluminum in SEM," *Journal of Japan Institute of Light Metals*, Vol. 46, No. 4, pp. 177~182.
- Heo, S. J., Kang, J. H. and Kim, W. I., 1993, "A Study on the High Efficiency Grinding of WC-Co," *KSME (A)*, Vol. 17, No. 3, pp. 721~730.
- Heo, S. J., Kang, J. H. and Kim, W. I., 1993, "A Study on the Grinding of WC-Co with High Quality," The 1st ICPMT International Conference.
- Technical Research Institute, 1997, *Machining Data Files* (Edited by Japan society for the Promotion of Machine Industry), Tokyo, 95-0321.
- Technical Research Institute, 1997, *Machining Data Files* (Edited by Japan society for the Promotion of Machine Industry), Tokyo, 95-0323.
- Technical Research Institute, 1997, *Machining Data Files* (Edited by Japan society for the Promotion of Machine Industry), Tokyo, 95-0325.
- Technical Research Institute, 1997, *Machining Data Files* (Edited by Japan society for the Promotion of Machine Industry), Tokyo, 92-0298.